Acta of Bioengineering and Biomechanics
Vol. 26, No. 3, 2024

Original paper
DOI: 10.37190/ABB-02517-2024-02

Evaluation of frictional wear in a follow-up screw-rod kinematic node in GGS transpedicular stabilization

JUSTYNA LICHOSIK, KLAUDIA SZKODA-POLISZUK*,
MAŁGORZATA ŻAK, CELINA PEZOWICZ

Department of Mechanics, Materials and Biomedical Engineering, Faculty of Mechanical Engineering,
Wrocław University of Science and Technology, Wrocław, Poland.

Purpose: The aim of this study was to evaluate the abrasive wear of the sliding screw-rod joint used in growth guidance system (GGS) stabilizers, allowing for the translation of the screw along the rod during the spinal growth process in a standard and modified system. *Methods*: The study used single kinematic screw-rod pairs made of titanium alloy Ti6Al4V. Mechanical tests (cyclic loads) simulated the stabilizer's operation under conditions similar to actual use. A microscopic evaluation was conducted, analyzing abrasive wear based on measured abrasion areas. Numerical simulations were performed for the standard joint system and for a structural change (an additional insert to increase contact area between the rod and sliding screw cap). *Results*: The study evaluated the abrasive wear of the mating elements of the stabilizer. Mechanical tests showed an increase in the force observed (11.74 ± 2.52 N) with the increasing number of load cycles. Microscopic evaluation showed abrasion of the caps and rods in two areas (upper and lower). Numerical simulations indicated the highest stresses in the standard system were on the mating elements, i.e., the rod and the cap (15.6 MPa). In the modified joint, stress distribution differed, concentrating on the surface of the insert and the rod, with maximum values of 6.0 MPa (PE insert) and 12.4 MPa (PEEK insert). *Conclusions*: Comparing the stress distributions obtained in the numerical simulations and the abrasive wear effects produced in the mechanical tests, a similar mechanism was observed (the destruction of the top layer of the mating elements of the stabilizer).

Key words: *GGS spinal stabilizers, experimental tests, cyclic loads, frictional wear, numerical simulations*

1. Introduction

Scoliosis, commonly known as lateral curvature of the spine, is a three-plane deformity occurring simultaneously in the frontal plane (with right thoracic curvature as a predominant type), sagittal plane (abnormalities of the physiological curvatures, i.e., thoracic kyphosis and lumbar lordosis), and horizontal plane (rotation and deformities within the vertebrae). Scoliosis is the most common orthopaedic condition among children and adolescents, occurring in 1–4% of patients [30]. The classification described by James in 1954 divides scoliosis into three groups: infantile scoliosis (for deformities occurring in children up to 3 years of age), juvenile scoliosis (in children between 3 and 10 years of age), and adolescent scoliosis (in children over 11 years of age) [12]. The first two groups (in which the curvature appears in children below 10 years of age) are referred to as early onset scoliosis (EOS). In young people, the disease is often caused by a congenital vertebral anomaly or neuromuscular abnormality. However, the most common case is idiopathic scoliosis of unknown aetiology. EOS is hard to treat, regardless of the aetiology of the curvature, as the aim of the treatment is not only to correct the deformity but also to slow the progression and allow for further growth of the thorax and spine. These measures can

* Corresponding author: Klaudia Szkoda-Poliszuk, Department of Mechanics, Materials and Biomedical Engineering, Faculty of Mechanical Engineering, Wrocław University of Science and Technology, Wrocław, Poland, e-mail: klaudia.szkoda-poliszuk@pwr.edu.pl
Received: September 23rd, 2024
Accepted for publication: October 10th, 2024

prevent serious health consequences, including the inability of the thorax to support breathing and proper lung development [8]. EOS can significantly reduce life expectancy compared to adolescent scoliosis. The treatment of children with early onset scoliosis is very difficult. Conservative (non-surgical) treatment is usually used first. In more severe cases, non-fusion surgery is performed, which postpones the fixation until the patient is older. In young patients, prolonged posterior fusion is avoided to prevent uneven growth of the trunk, which could result in pathological cardiac and respiratory changes [7]. The current focus in the treatment of EOS is to maximise growth of the spine and thorax using deformity control [36].

The development of implants that promote spinal growth has led to the replacement of early fixation and an approach that allows the skeleton to continue to grow unimpeded has become the preferred method of treatment [36]. In the treatment of deformities resulting from EOS, the main goal is to allow for correction of scoliosis while enabling the spine to grow uninhibited to skeletal maturity [20]. Mild to moderate deformities are corrected by medical means, with some cases requiring surgery. Methods of treating severe scoliosis in young patients include the distraction-based double-rod structures and growing rods (GRs) popularised by Akbarnia et al. [17]. Many researchers have confirmed the efficacy and safety of these systems while identifying the drawbacks. These types of stabilizers require periodic lengthening, which translates into repeated use of anaesthetics [3]. In addition, gradual stiffening of spinal segments has been reported along with a decrease in lengthening capacity [21], [26]. In response to the shortcomings of GRs, a new concept (Shilla Growth Guidance System – SGGS) has been developed to modulate spinal growth along parallel rods without the use of active distraction [17]. There are reports regarding the benefits of this system (a reduction in the overall number of operations compared to GRs) [19]. In a comparative study of both stabilizers [18], Shilla patients underwent three times fewer operations than GR patients. Despite its proven efficacy, the Shilla system has two main limitations: loss of correction and the need for osteotomy, which can cause serious complications [1]. Currently, the development of the Shilla system focuses primarily on structural modifications to reduce the problems referred to above. In addition to the above systems, Magnetically Controlled Growing Rods (MCGRs) are also popular [2]. They allow for a significant reduction in the number of surgical procedures using a percutaneous magnetic force (a magnet), which lets the rod to be lengthened non-invasively without re-surgery. This leads to a reduction in both revision surgery and complications (infections) [13].

Despite the proven effectiveness of such systems, there are some obstacles to overcome. One of the main problems is the abrasive wear between mating parts due to surface friction. Titanium and its alloys are considered to be relatively inert and biocompatible metals. However, if it remains in the body for several years, it can be gradually released into the surrounding tissues due to, among other things, corrosion processes and mechanical factors, such as friction or bending resulting from applied loads. Titanium can also enter the circulatory or lymphatic system in the form of nanoparticles, ions, organometallic complexes or oxides [28], [29]. This mechanism allows titanium to be transported to other tissues in the body. The released titanium can have a negative impact on bone remodelling processes and initiate acute and chronic inflammation. The properties of the materials are not always sufficient. Therefore, new solutions are sought (the structure itself is modified to include additional elements that increase the friction surface between the movable elements of the stabilizer [10] or additional coatings are used to increase abrasion resistance [22]). The aim of this study was to experimentally analyse changes (abrasive wear) occurring in the follow-up screw-rod kinematic node of a GGS stabilizer under long-term compressive loads. A new structural solution was also proposed: an additional insert to increase the contact area between the rod and the sliding screw cap. The stresses were determined in both standard and modified systems using numerical simulations and the finite element method.

2. Materials and methods

2.1. Material

The study used single kinematic screw-rod pairs of the GGS spinal stabilization system from NovaSpine (Domasław, Poland), comprising a transpedicular screw with a head, a blockade in the screw head, a sliding cap, and a rod (Fig. 1). The diameter of the screw was 6 mm and the length of the bone part was 40 mm. The sliding cap placed in the screw head was 4.5 mm long and 11 mm in diameter. The rod mating with the cap and screw had 100 mm in length and 5.5 mm in diameter. This type of joint is based on the mating of a rod placed in the screw head locked by a sliding cap which enables the screw to slide over the rod. The friction that

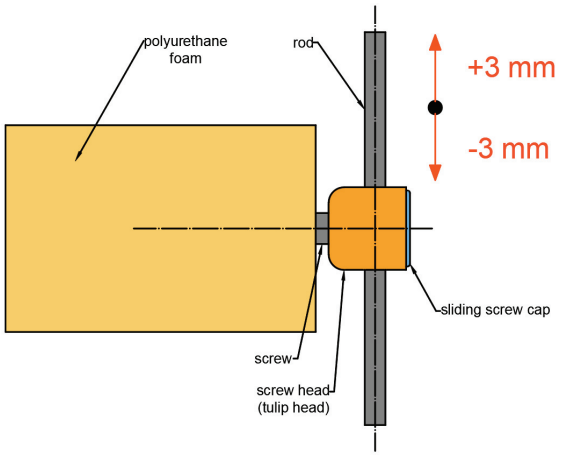

Fig. 1. Schematic diagram of the research system with elements of the kinematic pair: rod (∅ 5.5 mm, length 100 mm), transpedicular screw (∅ 6 mm, length of bone part 40 mm), and sliding screw cap (∅ 11 mm, length 4.5 mm). All elements were made of Ti6Al4V

occurs between the elements causes abrasive wear, which results in metal alloy particles being deposited on the tissues, causing inflammation. A sliding screw cap and a rod, both made of Ti6Al4V titanium alloy, were used. Each pair was placed in SYNBONE 30 PCF polyurethane foam with a density of 480.5 kg/m^3. This is the standard material used for mechanical testing using spinal implants due to its biomimetic reproduction that corresponds to vertebral bone tissue. Polyurethane foam of this density reproduces healthy bone tissue (*ASTM standard F1839-08*). A test group of four kinematic pairs was analysed.

Based on the actual dimensions of the implant, a three-dimensional (3D) geometric model of the sliding kinematic pair used in the experimental tests was developed in Autodesk Inventor Professional 2023 (Fig. 2a). Numerical studies were performed in ANSYS 2021 R1 using the finite element method (FEM). In addition,

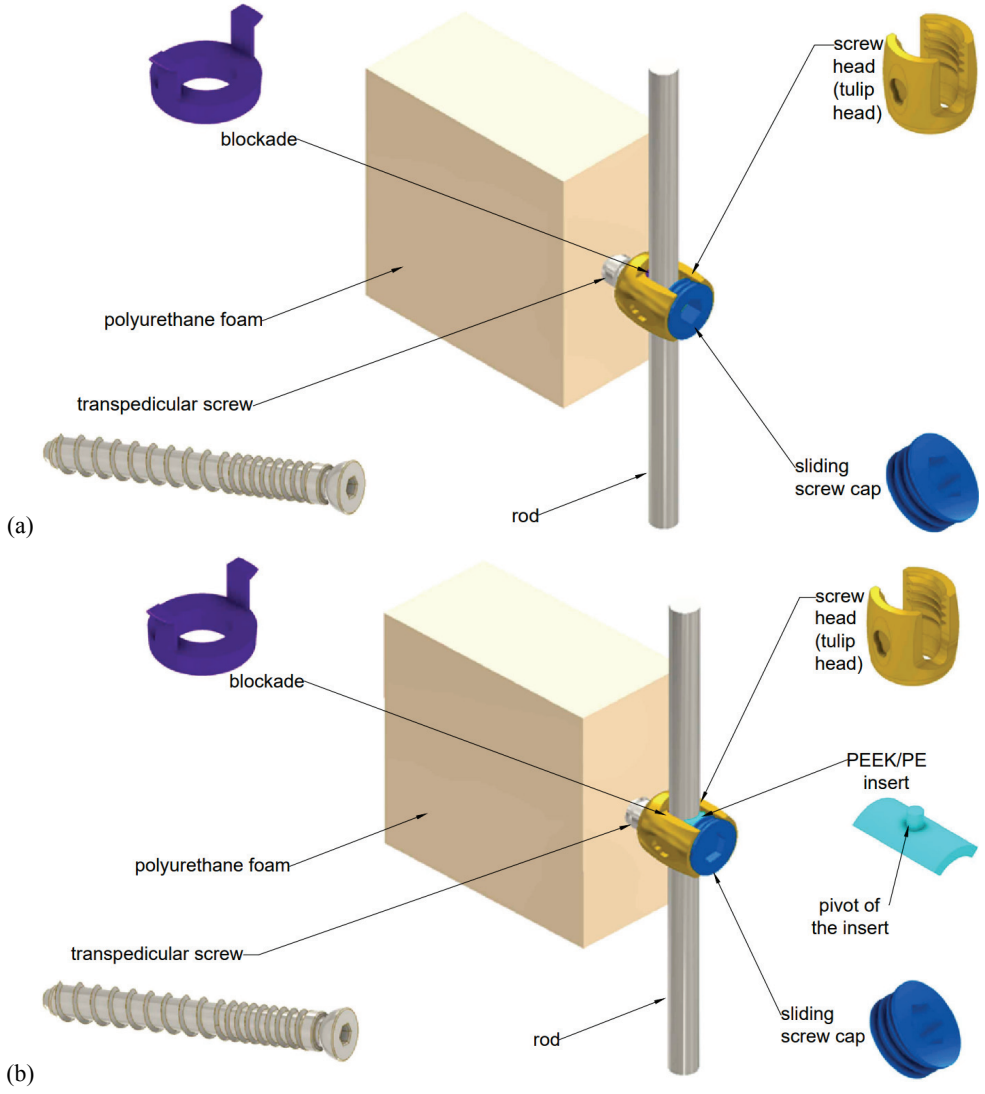

Fig. 2. Geometric model of a sliding kinematic pair made in Autodesk Inventor Professional 2023 with elements: rod, transpedicular screw with head and blockade, sliding screw cap, polyurethane foam: a) model without structural change; b) model with additional insert to provide a larger contact area between cap and rod

a structural change was proposed: an additional insert made of PEEK or PE to increase the contact area between the rod and the sliding cap (Fig. 2b).

The elements were given material parameters described by isotropic, linear elastic material properties (Table 1).

Table 1. Material data assigned to the kinematic pair elements

Model element	Material	Young's modulus [MPa]	Poisson's ratio [–]
Transpedicular screw	Ti6Al4V [31]	$1.14 \cdot 10^5$	0.37
Screw head			
Screw cap			
Blockade			
Rod			
Foam	PU [25] [ASTM standard F1839-08]	450	0.25
PE insert	PE [27]	1115	0.45
PEEK insert	PEEK [11]	3600	0.39

The friction coefficients needed to provide contact between elements were also determined (Table 2). In the kinematic pair model, the moving rod caused friction between the mating elements.

Table 2. Friction coefficients

Mating elements	Material	Friction coefficient [–]
Screw cap – Rod	Ti6Al4V – Ti6Al4V [24]	0.3
Blockade – Rod		
Screw head – Rod		
PE insert – Rod	PE – Ti6Al4V [33]	0.22
PEEK insert – Rod	PEEK – Ti6Al4V [15]	0.35

The discrete model is an important aspect of any numerical simulation and has an impact on the correctness of the calculations. A tetrahedral finite element mesh with a regular distribution was applied to the geometric models, with the size of one finite element being 1 mm. A three-dimensional ten-node higher-order element (Solid187) was chosen. It is suitable for modelling irregular meshes due to the three degrees of freedom at each node. The kinematic pair model without structural change was divided into 562.003 finite elements (Fig. 3a). The kinematic pair model with PE/PEEK insert was divided into 563.537 finite elements (Fig. 3b).

2.2. Methods

Mechanical tests (cyclic loads) were carried out to simulate the operation of the stabilizer under conditions similar to the actual operation of the elements.

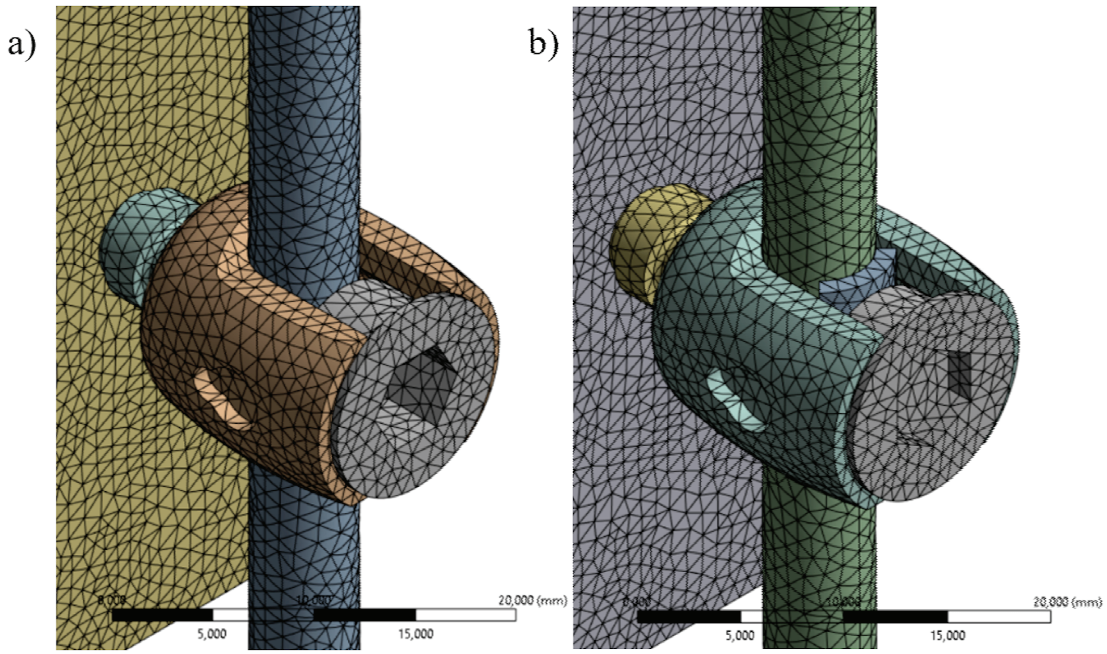

Fig. 3. Model of the kinematic pair: (a) without structural change, (b) with PE/PEEK insert with superimposed finite element mesh

100 000 load cycles [37] at a frequency of 2 Hz [4] were performed using an MTS Mini Bionix® 858 testing machine (MTS System, Eden Prairie, MN, USA). The rod was moved in the vertical axis by a value of ±3 mm (Fig. 1).

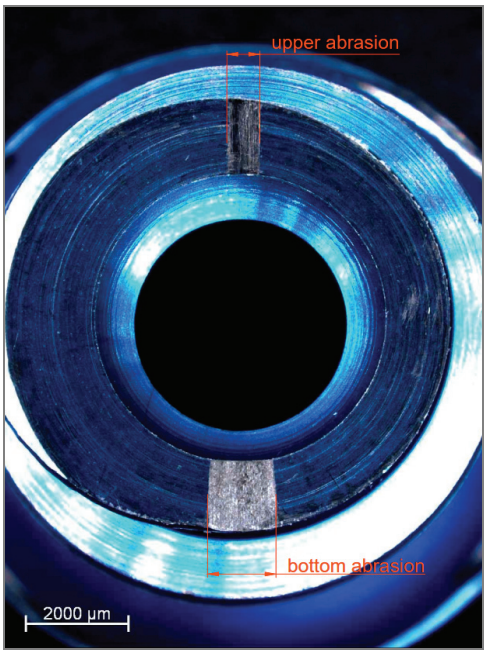

Fig. 4. Abrasive wear of standard N4 cap with marked measurement of upper and lower abrasion

The experimental tests were followed by microscopic tests to evaluate the abrasive wear on the surface of the caps and rods. The microscopic analysis was performed using a Zeiss Stereo Discovery V20 stereo microscope (Zeiss, Oberkochen, Germany). The amount of abrasive wear on the caps was measured using AxioVision Rel. 4.8 software. Upper and lower abrasion (Fig. 4) was measured at four locations in the center of the abrasion.

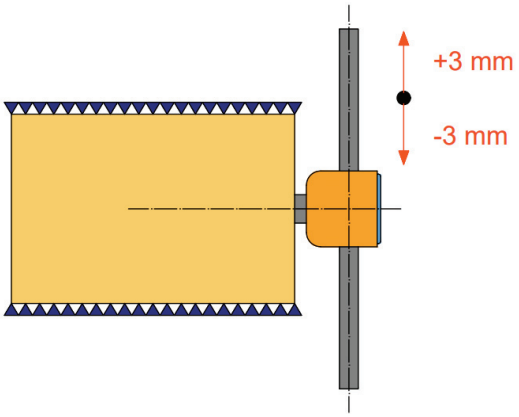

Fig. 5. Load model of the kinematic pair with marked restraint and load, i.e., displacement of the rod by ±3 mm in its long axis

At the final stage of the study, numerical simulations were carried out using the finite element method. For all combinations of kinematic pairs, numerical analysis was carried out. The displacement of the rod by ±3 mm in its long axis was controlled by reproducing the mechanical tests. The models were restrained by taking away all degrees of freedom of the lower and upper surfaces of the polyurethane foam (Fig. 5).

3. Results

3.1. Experimental tests

Graphs based on the results show the dependence of the maximum force on the number of loading cycles for various kinematic pairs. Characteristically, the force remains at 0.74 ± 0.15 N in the first 100 cycles and then increases to a maximum value of 10.1 ± 3.65 N. All kinematic pairs analysed showed a steadily increasing force with the increasing number of loading cycles. The increasing nature suggests that abrasive wear of the mating elements of the stabilizer occurred as the force increased. An example graph for the kinematic pair of cap N4 and rod P4 is shown below (Fig. 6).

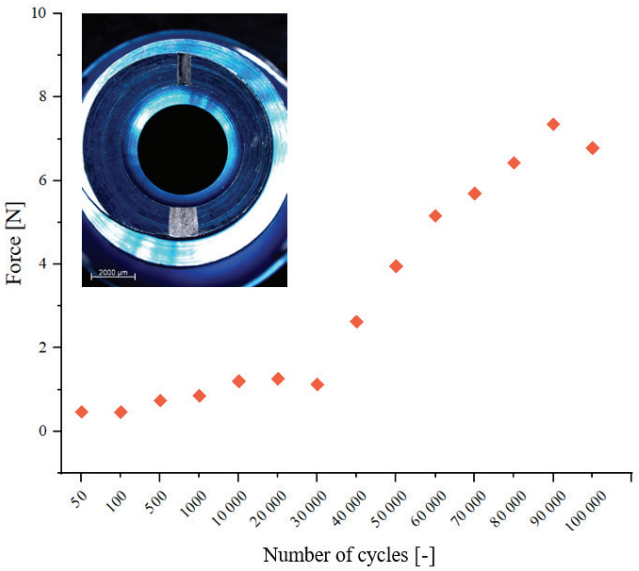

Fig. 6. Example characteristics of the dependence of the maximum force on the number of load cycles for the kinematic pair N4–P4

The average value of the force in successive cycles for all kinematic pairs is shown in Fig. 7. The analysis of the entire test group shows an increase in force with an increase in the number of load cycles. The characteristics obtained may be relevant in terms of the degree of abrasive wear of the mating elements.

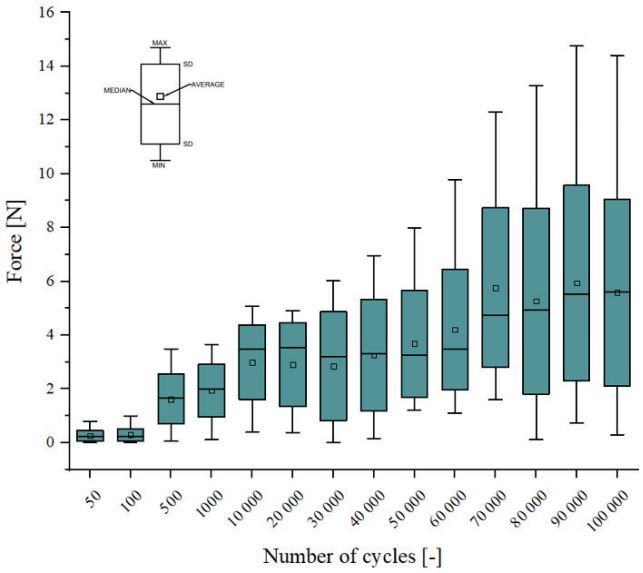

Fig. 7. Average value of the force in successive load cycles for all kinematic pairs

The mating of the cap-rod system resulted in abrasive wear visible on the surfaces of the mating elements. In Table 3, the average upper and lower abrasion widths for all caps and the standard deviation determined are shown. The average width of the upper abrasion is 784.4 ± 291.1 µm and the average width of the lower abrasion is 1267.3 ± 275.6 µm. The highest values were recorded for cap N1, with

Table 3. Abrasive wear of standard caps – average widths of upper and lower abrasion

Cap	Average width of upper abrasion [µm]	Average width of lower abrasion [µm]
N1	1280.9 ± 82.3	1600.9 ± 67.4
N2	613.7 ± 34.8	840.3 ± 57.5
N3	593.9 ± 12.8	1283.8 ± 42.9
N4	649.2 ± 19.9	1344.22 ± 27.3
Average	784.4 ± 291.1	1267.3 ± 278.6

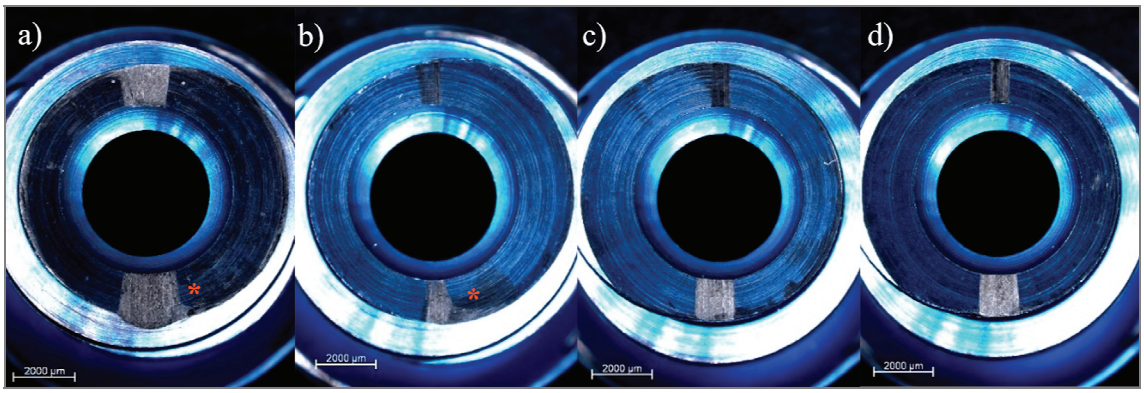

Fig. 8. Traces of abrasive wear of the caps: (a) N1, (b) N2, (c) N3, (d) N4; the asterisk marks the place of chipping of the material in caps N1 and N2

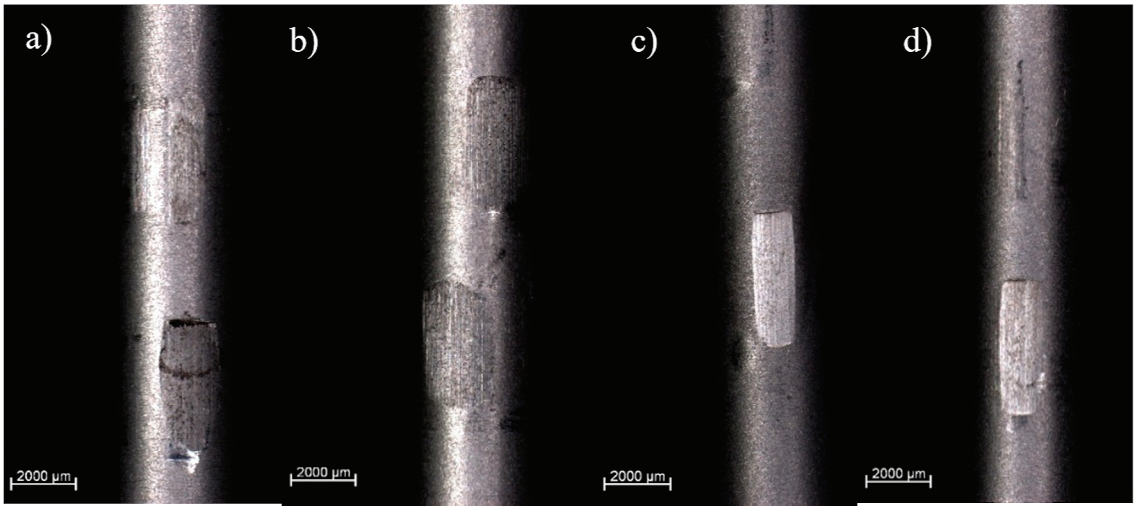

Fig. 9. Traces of abrasive wear of the rods: (a) P1, (b) P2, (c) P3, (d) P4

an upper abrasion width of 1280.9 ± 82.3 µm and a lower abrasion width of 1600.9 ± 67.4 µm. The highest forces were observed for the same kinematic pair, which may be a direct indication of increased wear and therefore greater abrasion. In all four cases, the size of the lower abrasion is larger than the upper one. In the case of caps N1 and N2, a small amount of material was chipped off at the bottom of the cap. Caps N3 and N4 suffered even wear with straight edges without any additional damage.

The photographs below show the traces of abrasive wear of the standard caps (Fig. 8) and the mating rods (Fig. 9).

3.2. Numerical simulations

The results for all models obtained from the numerical simulations were subjected to comparative analysis. For the analysed combinations, the distribution of reduced stresses according to the Huber–von Mises hypothesis was assessed. They were used to determine the abrasive wear of the mating elements and the effect of using an additional element to increase the contact area between the rod and the cap. The analysis covered the mating elements, i.e., the rod and the cap. In the case of kinematic pairs with

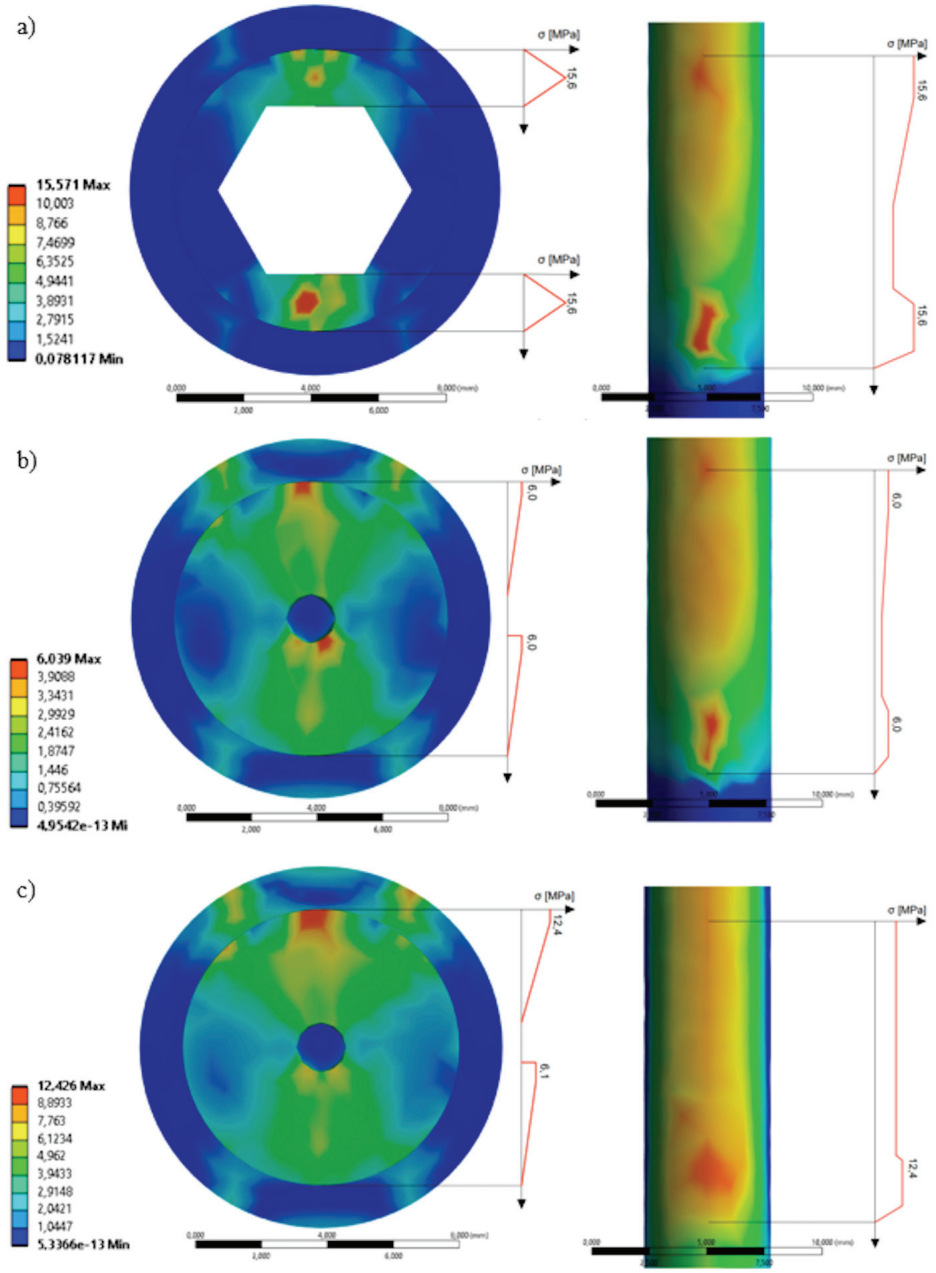

Fig. 10. Huber–von Mises stress distribution of the cap and the rod in the pair:
(a) without a structural change reproducing experimental tests, (b) with PE insert, (c) with PEEK insert

a structural change, the insert was additionally analysed.

In Figure 10a, the distribution of the reduced stresses according to the Huber–von Mises hypothesis for the cap and rod, the kinematic pair reproducing the experimental tests is shown. Increased stresses of approximately 16 MPa can be seen at the top and bottom of the cap, corresponding to the upper and lower abrasion (Fig. 8), which occurred in the experimental tests for this group. The stress concentration areas reproduce the actual operation of this joint. This is the contact area between the rod and the cap. Their movement fit causes increased wear at these areas. It can be seen that a larger area of stress concentration occurs at the bottom of this element. In contrast to the kinematic pair without structural change, the rod in the other models mated directly with the insert and not the cap. The cap had an additional hole in which the insert pin was placed. In both cases, stress concentrations were observed around the pin hole. The stresses reach up to 6 MPa in the model with the PE insert (Fig. 10b) and up to 12 MPa in the pair with the PEEK insert (Fig. 10c). In the kinematic pair reproducing the experimental tests, the highest stresses for the rod were recorded at the contact points with the cap. Two areas of stress concentration were observed: at the contact points of the top and the bottom with the cap. The maximum values (approximately 16 MPa) are located at the bottom of this element (Fig. 10a). The kinematic pairs with the structural change have a different distribution. The stresses are distributed in the area resulting from the contact between the rod and the additional insert. The kinematic pair with the PEEK insert showed lower stresses (approximately 12 MPa) (Fig. 10c). Similarly, in the case of the model with the PE insert, the highest stresses (approximately 6 MPa) are located in one small area resulting from the contact between the elements (Fig. 10b).

The distribution of reduced stresses according to the Huber–von Mises hypothesis of the PEEK and PE inserts is shown in Fig. 11. The analysis of both elements shows that stress concentrations occur in the central part of the insert along its entire length. The stresses are also located on the other side, around the pin that allows the element to be mounted. The maximum values reach approximately 13 MPa for the kinematic pair with PEEK insert and approximately 4 MPa for the model with PE insert. Their distribution is strongly related to the operation of the element. It mates with the moving rod. Visible areas of concentration could indicate the formation of abrasive wear at this location.

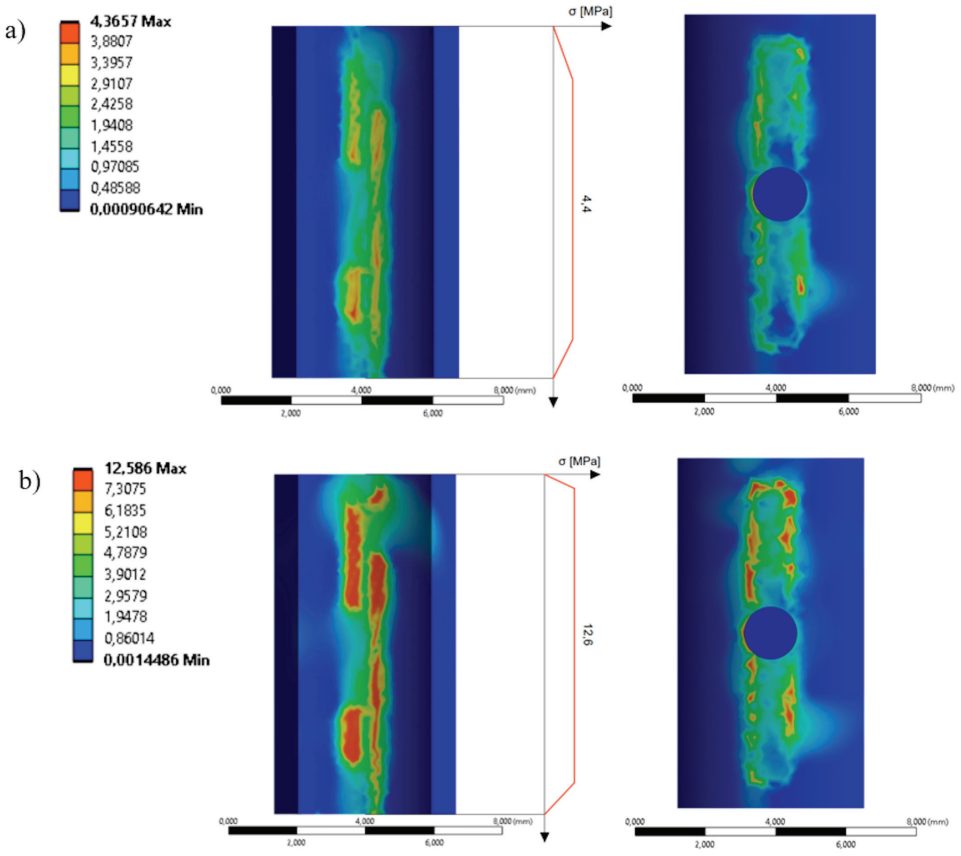

Fig. 11. Huber–von Mises reduced stress distribution for: (a) PE insert, (b) PEEK insert

4. Discussion

The analysis of the kinematic joint between the screw and rod of the GGS spinal stabilizer allowed the evaluation of abrasive wear occurring during long-term cyclic loads. Experimental tests showed an increasing nature of the force with the increasing number of loading cycles. In the first 100 cycles, a slight change in force is observed, which can be directly related to the clearance fitting between the rod and the cap. After 100 cycles, there is a successive increase in force, which may be indicative of an ongoing friction process and increasing abrasive wear of the material. The force values had an upward trend. The stabilization of the force occurred after about 10 000 cycles of movement and the values had a sharp upward trend after about 50 000 cycles. On the basis of the numerical simulations, the stress distribution was determined, especially the areas with higher values of this parameter on various elements of the stabilizer. In the standard pair, two areas of stress concentration are evident, i.e., on the top and bottom surfaces of the cap and on the corresponding areas on the surface of the support rod, where higher values were observed in the lower part of both the rod and the cap. The experimental tests showed the same pattern of changes. One of the reasons for the higher friction losses may have been the change in position of the tulip head, which descended (under the influence of gravity) resting on the rod by way of the bottom surface of the cap. The polyaxial screws used in the study have the ability to change the position of the tulip (screw head) in relation to the shaft, thus allowing the angle between the rod and the screw to be altered. In classic spinal stabilizers, once the polyaxial screws are inserted and the supporting rods are fitted to them, the cap is finally and permanently tightened and the final position of the stabilizer is established. In GGS systems, the sliding screw cap is fixed in a position that allows for free movement of the rod relative to the screw and the change of the position of the head. The randomness of the positioning of the polyaxial screw's tulip relative to the rod may have influenced the distribution of wear on the surface of the caps and rods. The geometry of the transpedicular screw thread also has an important influence on the phenomena occurring at the contact points between the screw thread vs. screw head and screw vs. bone tissue [23]. As shown by the results of numerical simulations, the screw with the head is bent under the influence of the displacement of the rod and the rod rests on the opposing areas of the contact point between the cap or washer vs. head, which directly translates into stress concentration points on the rod and smaller stresses along its length. These areas can be places with increased abrasive wear. In this study, the traces of abrasive wear caused by the friction on the surfaces of the sliding screw caps in the area of contact with the rod had different shapes (which was confirmed by measurements of the width of the wear traces and the observed areas of material chipping). In all cases analysed, the size of the lower abrasion was larger than the upper one. Unfortunately, it is very difficult to obtain a uniform distribution of rod pressure on the cap surface. The variation in the shapes of the wear traces may indicate the presence of different types of contact in the follow-up screw-rod kinematic node. On the friction surfaces, a mechanism of abrasive wear (scratching and chasing) was observed. In addition, different friction conditions (the appearance of a certain amount of wear products with irregular geometries) may also have occurred, which influenced the rate and nature of wear on these elements.

Demir et al. [10] investigated five different spinal stabilization systems using transpedicular screws and showed that these types of mechanisms are susceptible to fatigue failure at the contact point between the supporting rods and the screw head vs. cap. The cyclic loads caused the rod to fracture at the contact point with the cap, which has also been observed in other papers [6], [13]. The small contact area between the screw and the rod as well as the high stiffness of the system (also dependent on the configuration of the stabilization system [32]) resulted in a high stress concentration in this area, which initiated the formation of cracks leading to screw fracture. A new cap was therefore developed with an additional element with a larger contact area to reduce the stress concentration. Based on the results of bending and fatigue tests, a friction force was determined. The force was significantly higher compared to the standard concept, which was related to the increased contact area between the insert and the rod. A threefold improvement in fatigue strength was also observed. In contrast to the present study conducted by the authors, which was limited to 100 000 cycles, the study by Demir et al. [10] covered a larger number of cycles (as many as 5 million). Therefore, it is difficult to directly compare the results.

In this study, a similar solution was proposed in the numerical analysis: an additional insert to increase the contact area between the rod and the sliding screw cap. Two different materials (PEEK and PE), which turned out to influence the results, were proposed. PEEK is a polymer widely used as a frictional wear-reducing material [15] due to its favourable tribological proper-

ties, with a friction coefficient of 0.4 [16], a high tensile strength of 100 MPa [35] and a Young's modulus of 3600 MPa [11]. It is also a stiff material, which may cause it to chip under long-term cyclic loads. PE is a material with good mechanical strength, a Young's modulus of 1115 MPa and a tensile strength of 45 MPa [27]. It has a friction coefficient of 0.2 [34], making it a good choice for applications requiring long-term durability. The choice of material for implant components is a compromise between different properties and the decision depends on many factors. The structural modification used in the numerical simulations resulted in a different stress distribution and the stress area was much larger and covered the entire length of the insert. In the PEEK insert model, the stresses observed were higher than in the PE insert model (approximately 13 MPa and 4 MPa, respectively). Comparing these values to the yield strength of both materials (75 MPa for PEEK [14] and 25 MPa for PE [9]), both proposals met the strength requirements at the given load. Joints of this type in GGS stabilizers are based on the mating of several elements and frictional contacts occurring between adjacent titanium elements can lead to adverse phenomena, i.e., material wear. To avoid potential side effects caused by metallic abrasive wear products, it is worth modifying existing structures by reducing the frictional force between sliding rods and screws. Titanium alloys are characterised by low resistance to frictional wear, a tendency to chipping, and a high friction coefficient (0.4) [5]. Their high strength parameters (tensile strength of 860 MPa and Young's modulus of 114 GPa [31]) are not always sufficient and suitable for the needs, which is why plastics are increasingly used as sliding materials, as an alternative to their metallic counterparts.

The existing research and analysis have some limitations, e.g., due to the research methods used or the size of the research sample. Experimental tests were performed under laboratory conditions without taking into account the complex conditions of the tissue environment, and the operation of the stabilizer was replicated under dry friction conditions. Although laboratory conditions allow for more precise control of many variables than those found in the actual implantation procedure, there are some limitations. First of all, during a series of mechanical tests involving 100 000 load cycles, the possibility of displacement of the tulip of the polyaxial transpedicular screw relative to the rod was observed. The displacement could have caused a certain variation in the results around the mean value of the force obtained. The size of the experimental group was limited, which could also have influenced the results. Therefore, further studies (on an extended test group, including in an aqueous environment and for different insert solutions) are planned. The numerical simulations based on the finite element method are a certain simplification of the experimental tests. The simulation did not reproduce the actual environment of operation of the stabilizer elements, such as temperature or humidity. The studies carried out so far may have an impact on the development of spinal stabilization systems using transpedicular screws as well as other implants. Many studies are based on the use of mating elements, with the friction between them being the main mechanism leading to implant failure.

5. Conclusions

The results obtained lead to the following conclusions:

- the long-term cyclical loads acting on the system cause abrasive wear of the mating elements and the appearance of wear products, which can lead to the development of inflammation in the surrounding tissues;
- microscopic analysis showed that different shapes of the abrasive wear traces can be influenced by a large number of factors resulting from the relative position of the elements of the posterior fixation system, with the randomness of the position of the tulip relative to the rod being the main factor;
- the numerical simulations showed stress concentrations in areas that may indicate increased tribological wear;
- the modification of the structure changed the stress distribution on the mating elements and the use of susceptible materials reduced the stresses present in the system.

Acknowledgements

The research results have been carried out as part of the research task "Evaluation of the degree of frictional wear at the border of the sliding screw-rod joint used in spinal stabilizers" financed from the pro-quality subsidy for the development of research potential of the Faculty of Mechanical Engineering at Wrocław University of Science and Technology in 2022.

References

[1] AGARWAL A., AKER L., AHMAD A.A., *Active Apex Correction With Guided Growth Technique for Controlling Spinal Deformity in Growing Children: A Modified SHILLA Technique*, Global Spine Journal, 2019, DOI: 10.1177/2192568219859836.

[2] AHMADA A.A., AGARWAL A., *Active Apex Correction: An overview of the modified SHILLA technique and its clinical efficacy*, Journal of Clinical Orthopaedics and Trauma, 2020, 11, 848e852, DOI: 10.1016/j.jcot.2020.07.013.

[3] BESS S., AKBARNIA B.A., THOMPSON G.H., SPONSELLER P.D., SHAH S.A., EL SEBAIE H., BOACHIE-ADJEI O., KARLIN L.I., CANALE S., POE-KOCHERT C., SKAGGS D.L., *Complications of growing-rod treatment for early-onset scoliosis: Analysis of one hundred and forty patients*, Journal of Bone and Joint Surgery, 2010, Vol. 92, Issue 15, 2533–25433, DOI: 10.1186/s13018-021-02267-y.

[4] BOBER T., *Biomechanics of walking and running*, Studies and Monographs of the AWF in Wrocław, Workbook No. 8, Wrocław 1985.

[5] CHEN Q., ZHANG J., HUANG A., WEI P., *Study on Wear Resistance of Ti-6Al-4V Alloy Composite Coating Prepared by Laser Alloying*, Appl. Sci., 2021, 11 (1), 446, DOI: 10.3390/app11010446.

[6] CRYAR K.A., BUMPASS D.B., MCCULLOUGH L., MCCARTHY R.E., *Rod breakage in Shilla growth guidance constructs: when, where, and why?*, Spine Journal, 2017, 17 (10), S107, DOI: 10.1016/j.spinee.2017.07.091.

[7] CUNIN V., *Early-onset scoliosis – Current treatment*, Orthopaedics and Traumatology: Surgery and Research, 2015, Vol. 101, Iss. 1, Suppl., S109–S118, DOI: 10.1016/j.otsr.2014.06.032.

[8] DANIELEWICZ A., WÓJCIAK M., SAWICKI J., DRESLER S., SOWA I., LATALSKI M., *Comparison of different surgical systems for treatment of early-onset scoliosis in the context of release of titanium ions*, Spine, 2021, 46 (10), E594–E601, DOI: 10.1097/BRS.0000000000003846.

[9] FARZI A., DEHNAD A., SHIRZAD N., NOROUZIFARD F., *Biodegradation of high density polyethylene using Streptomyces species*, Journal of Coastal Life Medicine, 2017, 5 (11), 474–479, DOI: 10.12980/jclm.5.2017J7-94.

[10] DEMIR T., CAMUSCU N., *Design and performance of spinal fixation pedicle screw system*, Sage Journals, 2011, DOI: 10.1177/0954411911427351.

[11] JAHNG T., KIM Y.E., MOON K.Y., *Comparison of the biomechanical effect of pedicle-based dynamic stabilization: a study using finite element analysis*, The Spine Journal, 2013, 13, DOI: 10.1016/j.spinee.2012.11.014.

[12] LATALSKI M., FATYGA M., KOŁTOWSKI K., MENARTOWICZ P., REPKO M., FILIPOVIČ M., *"Guided growth" implants in the treatment of early childhood scoliosis. Preliminary report*, Orthopaedics Traumatology Rehabilitation, 2013, 1 (6), Vol. 15, 23–29, DOI: 10.5604/15093492.1032798.

[13] LEBON J., BATAILLER C., WARGNY M., CHOUFANI E., VIOLAS P., FRON D., KIEFFER J., ACCADBLED F., CUNIN V., SALES DE GAUZY J., *Magnetically controlled growing rod in early onset scoliosis: a 30-case multicenter study*, Eur. Spine J., 2017, DOI: 10.1007/s00586-016-4929-y.

[14] LIAO CH., LI Y., TJONG S.Ch., *Polyetheretherketone and Its Composites for Bone Replacement and Regeneration*, Polymers, 2020, 12 (12), 2858, DOI: 10.3390/polym12122858.

[15] LIN L., ZHAO Y., HUA C., SCHLARB A.K., *Effects of the Velocity Sequences on the Friction and Wear Performance of PEEK-Based Materials*, Tribology Letters, 2021, DOI: 10.1007/s11249-021-01452-8.

[16] LIN Z., YUE H., GAO B., *Enhancing tribological characteristics of PEEK by using PTFE composite as a sacrificial tribofilm-generating part in a novel dual-pins-on-disk tribometer*, Wear, 2020, Vol. 460–461, DOI: 10.1016/j.wear.2020.203472.

[17] LUHMANN S.J., SMITH J.C., MCCLUNG A., MCCULLOUGH F.L., MCCARTHY R.E., THOMPSON G.H., *Growing Spine Study Group, Radiographic Outcomes of Shilla Growth Guidance System and Traditional Growing Rods Through Definitive Treatment*, Spine Deformity, 2017, Vol. 5, Issue 4, 277–282, DOI: 10.1016/j.jspd.2017.01.011.

[18] MCCARTHY R., BUMPASS D.B., *Shilla Growth Guidance Technique for Early Onset Scoliosis*, Journal of Bone and Joint Surgery, 2015, DOI: 10.2106/JBJS.N.01083.

[19] MCCARTHY R., LENKE L., LUHMANN S., *Do growth guidance rods have acceptable complications and fewer surgeries?*, San Antonio Texas: Scoliosis Research Society, 2009.

[20] MORELL S.M., MCCARTHY R.E., *New developments in the treatment of early-onset spinal deformity: role of the Shilla growth guidance system*, Medical Devices: Evidence and Research, 2016, DOI: 10.2147/MDER.S77657.

[21] NOORDEEN H.M., SHAH S.A., ELSEBAIE H.B., GARRIDO E., ENRIQUE, FAROOQ N., AL-MUKHTAR M., *In vivo distraction force and length measurements of growing rods: which factors influence the ability to lengthen?*, Spine, 2011, DOI: 10.1097/BRS.0b013e31821b8e16.

[22] PAN Y.P., DON J., CHU T.P., MAHAJAN A., *Influence of Diamond – like Carbon coatings on the fatigue behawior of spinal implant rod, Time Dependent Constitutive Behavior and Fracture/Failure Processes*, Vol. 3: Proceedings of the 2010 Annual Conference on Experimental and Applied Mechanics, 383–389, DOI: 10.1007/978-1-4419-9794-4_53.

[23] PEZOWICZ C., FILIPIAK J., *Influence of loading history on the cervical screw pullout strength value*, Acta of Bioengineering and Biomechanics, 2009, 11, 3, 35–40.

[24] SAIDEEPAK R., *Inspection of cp titanium material and its coefficient of friction*, International Research Journal of Engineering and Technology, 2021, Vol. 08, Issue: 02.

[25] SANBORN B., SONG B., *Poisson's Ratio of a Hyperelastic Foam Under Quasi-static and Dynamic Loading*, International Journal of Impact Engineering, 2018, DOI: 10.1016/j.ijimpeng.2018.06.001.

[26] SANKAR W.N, SKAGGS D.L., YAZICI M., JOHNSTON C.E., SHAH S.A., JAVIDAN P., KADAKIA R.V., DAY T.F., AKBARNIA B.A., *Lengthening of dual growing rods and the law of diminishing returns*, Spine, 2011, Vol. 36, Issue 10, 806–8091, DOI: 10.1097/BRS.0b013e318214d78f.

[27] SARAMBALE D.S., SHINDE D.K., *Electro-fusion joint failure polyethylene pipes analysis and its simulation using finite element analysis*, International Journal of Mechanical and Production Engineering, 2017, Vol. 5, Iss. 12.

[28] SARMIENTO-GONZALEZ A., ENCINAR J.R., MARCHANTE-GAYO´N J.M. et al., *Titanium levels in the organs and blood of rats with a titanium implant, in the absence of wear, as determined by double-focusing ICP-MS*, Anal. Bioanal. Chem., 2009, 393, 335–343, DOI: 10.1007/s00216-008-2449-2.

[29] SAWICKI J., WOJCIAK-KOSIOR M., STANIAK M. et al., *Biocompatibility and biotolerability of titanium-based material used in medicine*, TEKA Arch. Comm. Med. Sci., 2017, 1, 57–59.

[30] SKAGGS D.L., GUILLAUME T., EL-HAWARY R., EMANS J., MENDELOW M., SMITH J., *Early onset scoliosis consensus statement*, SRS Growing Spine Committee, 2015, Spine Deformity, 2015, 3, 107, DOI: 10.1016/j.jspd.2015.01.002.

[31] SURMA K., ADACH M., DĘBOWSKA M., TURLEJ P., SZYMCZYK P., *Design and computational analysis of a cervical spine intervertebral disc for fabrication using incremental technologies*, Current Problems in Biomechanics, 2019.

[32] SZKODA-POLISZUK K., ŻAK M., ZAŁUSKI R., PEZOWICZ C., *Biomechanical Analysis of the Impact of Transverse Connectors of Pedicle-Screw-Based Fixation on Thoracolumbar*

Compression Fracture, Applied Sciences, 2023, 13 (24), 13048, DOI: 10.3390/app132413048.

[33] TETREAULT D.M., KENNEDY F.E., *Friction and wear behavior of ultrahigh molecular weight polyethylene on Co-Cr and titanium alloys in dry and lubricated environments*, Wear, 1989, DOI: 10.1016/0043-1648(89)90043-4.

[34] WRÓBEL G., SZYMICZEK M., *Influence of temperature on friction coefficient of low density polyethylene*, Journal of Achievements in Materials and Manufacturing Engineering, 2008, Vol. 28, Iss. 1.

[35] WU W., GENG P., LI G., ZHAO D., ZHANG H., ZHAO J., *Influence of Layer Thickness and Raster Angle on the Mechanical Properties of 3D-Printed PEEK and a Comparative Mechanical Study between PEEK and ABS*, Materials, 2015, 8, 5834–5846, DOI: 10.3390/ma8095271.

[36] YANG S., ANDRAS L.M., REDDING G.J., SKAGGS D.L., *Early-onset scoliosis: A review of history, current treatment, and future directions*, Pediatrics, 2016, DOI: 10.1542/peds.2015-0709.

[37] ŻAK M., *Effect of support on mechanical properties of the intervertebral disc in long-term compression testing*, Journal of Theoretical and Applied Mechanics, 2014, 52 (3), 677–686.